Anomalous In-plane Magnetoresistance of Electron-doped Cuprate $La_{2-x}Ce_xCuO_{4\pm\delta}$

H. S. Yu[1], G. He[1], Y. L. Jia[1], X. Zhang[1], J. Yuan[1], B. Zhu[1], A. Kusmartseva[3], F. V. Kusmartsev[3], and K. Jin[1,2,*],

[1]*Beijing National Laboratory for Condensed Matter Physics, Institute of Physics, Chinese Academy of Sciences, Beijing 100190, China*

[2]*Collaborative Innovation Center of Quantum Matter, Beijing, 100190, China*

[3]*Department of Physics, Loughborough University, Loughborough LE11 3TU, United Kingdom*

We report the systematic in-plane magnetoresistance measurements on the electron-doped cuprate $La_{2-x}Ce_xCuO_{4\pm\delta}$ thin films as a function of doping and oxygen content in the magnetic field up to 14 T. A crossover from negative to positive magnetoresistance occurs between x = 0.07 and 0.08. Above x = 0.08, the positive magnetoresistance effect emerges, and is almost indiscernible at x = 0.15. By tuning the oxygen content, the as-grown samples show negative magnetoresistance effect, whereas the optimally annealed ones display positive magnetoresistance effect at the doping level x = 0.15. Intriguingly, a linear-in-field magnetoresistance is observed at both the underdoped doping level x = 0.06 and the optimal doping level x = 0.10. These anomalies of in-plane magnetoresistance may be related to the intrinsic inhomogeneity in the cuprates, which can be understood in the framework of network picture.

In order to understand the high-T_c superconductivity in the cuprates, it is necessary to study the unusual properties of the normal state by suppressing the superconductivity with magnetic field. Till now, many investigations of magnetoresistance (MR) are focused on the hole-doped cuprates to study properties of the normal state, i.e. the topology of Fermi Surface[1,2], quantum criticality[3] etc. Compared with hole-doped cuprates, it is much easier to quench the superconductivity to study the normal state behaviors in the electron-doped counterpart[4]. Recently, low temperature negative MR (*n*-MR) effect was found in underdoped region of $Pr_{2-x}Ce_xCuO_{4\pm\delta}$ (PCCO), $Nd_{2-x}Ce_xCuO_{4\pm\delta}$ (NCCO) and $La_{2-x}Ce_xCuO_{4\pm\delta}$ (LCCO) in the case of B (magnetic field)$\perp ab$ plane (i.e. CuO_2 plane)[5-7]. The origin of *n*-MR was attributed to two-dimensional weak localization, Kondo scattering, etc. Meanwhile, an upturn in temperature dependence of resistivity in the underdoped regime and metal-to-insulator transition near the optimal doping level were suggested to be related to the appearance of antiferromagnetic order with reducing temperature and doping, respectively[5,8,9]. When B//ab plane, the in-plane MR showed two-fold symmetry in LCCO and coexistence of two- and four-fold symmetries in PCCO and NCCO, both pointing to the antiferromagnetic order[10-12]. Neutron and transport studies on $Pr_{1.3-x}La_{0.7}Ce_xCuO_{4\pm\delta}$ (PLCCO) revealed that the four-fold symmetric angular dependence is caused by a spin-flop transition, where the MR decreases as B//Cu-Cu direction, but increases as B//Cu-O-Cu direction[13]. Intriguingly, in both $B\perp ab$ plane and B//ab plane, a linear-in-field MR was observed at certain doping levels in PCCO, NCCO and LCCO systems[10,14,15]. But the origin of the linearity is still under debate[16]. In addition to Ce doping, tuning oxygen by varying annealing procedures also has remarkable influence on the properties of normal state[17,18]. For instance, the crossover from *n*-MR to positive MR (*p*-MR) was found by reducing the oxygen contents in NCCO[19,20]. Meanwhile the antiferromagnetic order fades away with increasing the annealing time[11,21].

Although fruitful MR anomalies in normal state of electron-doped cuprates have been unveiled, a systemic study on MR effects as a function of temperature, Ce, as well as oxygen in one system is still lacking. In this paper, we present the in-plane MR of LCCO thin films in a wide range of Ce doping levels and oxygen content when $B//ab$ plane. At x = 0.06 and 0.07, the optimally annealed samples exhibit n-MR. The crossover from n-MR to p-MR occurs between x = 0.07 and 0.08. By varying the annealing processes, the in-plane MR of LCCO at x = 0.15 changes from n-MR (as-grown samples) to p-MR (the optimally annealed samples). Intriguingly, the linear MR is observed at the underdoped doping level x = 0.06 and the optimal doping level x = 0.1. All the results are summarized in the phase diagram (see in Fig.4). These MR behaviors may be interpreted by the existence of a network in the LCCO thin films[22].

All the (00l) $La_{2-x}Ce_xCuO_{4\pm\delta}$ thin films were deposited directly on the $SrTiO_3$ substrates by the pulsed laser deposition technique at 700 ~ 750℃ (ref.10). To achieve the highest T_{c0} (zero-resistance superconducting transition temperature) and sharpest transition width for different doping levels, we carefully adjusted the annealing process after deposition. Then all the thin films (2000Å) were patterned into Hall-bar shape and measured in a Quantum Design PPMS 14T magnet at different angles between magnetic field and the current (I). Measurements were taken with B//ab plane at 35 K due to the occurrence of superconducting fluctuations below 30 K and the large in-plane upper critical field[23,24]. By changing the annealing time, samples of different oxygen contents can be obtained.

Figure 1 displays the in-plane MR of LCCO thin films at 35 K with the Ce doping levels x = 0.06, 0.07, 0.08, 0.1, 0.11 and 0.15, respectively. In Fig. 1(a) and (b), the optimally annealed samples show n-MR at x = 0.06 and 0.07. The crossover from n-MR to p-MR occurs between x = 0.07 and 0.08, in accordance with the boundary of long-range antiferromagnetic order achieved by low energy μSR probe[25]. With further increasing Ce doping, the p-MR becomes indiscernible at x = 0.15 in Fig. 1 (c) ~ (f).

In Fig.2, the in-plane MR is plotted as a function of magnetic field at the doping level x = 0.15 subject to different annealing processes. In Fig.2(a), when the angles between the current and magnetic field are 0^o ($B//I$) ,45^o and 90^o ($B\perp I$), the as-grown samples always show n-MR at 10 K. However, the short-annealed samples exhibit n-MR in low magnetic field but p-MR above 13 T in Fig.2(b). For the optimally annealed samples, the in-plane MR shows p-MR in the case of $B//I$ and $B\perp I$ (Fig.1(f)). The crossover from n-MR to p-MR is also observed by varying annealing process.

Intriguingly, negative linear field dependence in MR is seen at the underdoped doping level x = 0.06 at 35 K (Fig.1(a)). Similarly, positive linear in-plane MR occurs at the optimal doping level x = 0.1 in Fig.1(e). The enigma of the linear in-plane MR of x = 0.1 is thoroughly investigated at $\theta = 30^o, 45^o, 60^o$, and 90^o, as shown in Fig.3. Surprisingly, when the magnetic field was normalized by a sine function of the angle θ, the linear in-plane MR converged on a single straight line (shown in the inset of Fig.3). This means that for linear MR only the perpendicular component of the field to the current direction is significant. Similar phenomena are also observed in other electron-doped cuprates. For example, in PCCO and NCCO systems, the negative linear MR happens in the underdoped regime[14,15]. Meanwhile, near the optimal doping level, the samples show positive linear MR in PCCO system[26].

Our findings can be summarized as follows: first, the crossover from n-MR to p-MR occurs between the doping level x = 0.07 and x = 0.08, in accordance with the boundary of long-range antiferromagnetic order achieved by μSR (ref.25). Second, similar crossover occurs by varying annealing process. Third, the linear MR is observed at the doping level x = 0.06 and x = 0.1. Next, we will focus on two fundamental phenomena: n-MR and linear MR.

All the in-plane MR $\Delta\rho = \alpha B^{\gamma}$ in LCCO thin films are summarized in the Fig.4. In the lightly doping regime, where the long-range antiferromagnetic order exists, the optimally annealed samples exhibit *n*-MR (shown by the blue area in Fig.4), which may be related to the conducting nano-filament (CNF) network model used to describe the properties of normal state in the electron-doped cuprates[22]. Doping the electron into the CuO_2 plane will result in creation of spin-orbital (SO) polarons associated with polarization of orbitals. These polarons are similar to ferrons in antiferromagnetic semiconductor originally introduced by Nagaev[27]. The SO polarons have a tendency to form clouds (or SO strings) inside of antiferromagnetic background, which may have a quasi-one dimensional character to decrease the Coulomb repulsion between doped electrons inside the cloud[28-30]. The doped electron could move along the one-dimensional channel inside these clouds of SO polarons. Owing to a small quantity of polorans, the long-range antiferromagnetic order could be stable up to the critical doping level $x = 0.08$. Note that antiferromagnetic order as well as the magnetic moment associated with the clouds is in the plane. The tunneling of the polarons between different planes is very rare event. Therefore, before the long-range antiferromagnetic order is destroyed, spins or magnetic moments inside these clouds of SO polarons are polarized due to the magnetic field. Such polarization decreases the spin scattering. As a result, the *n*-MR effect occurs. It is similar to the *n*-MR behaviors in high magnetic field as $B \perp ab$ plane[31]. The *n*-MR signals are also very weak due to two reasons: a strong antiferromagnetic background where spins are located in the plane and a small number of SO polarons which form droplets decoupled from each other by antiferromagnetic background.

With doping the SO polarons will also form a depletion that erases the interaction links in the antiferromagnetic lattice, and therewith weaken the antiferromagnetic interaction both between the planes and inside them. With increasing doping level, there appear more and more erased moments. This frustration leads to the antiferromagnetic decoupling of planes from each other arising at some critical dopings. Then, due to these frustrations the long-range antiferromagnetic order is vanishing at the critical doping level $x = 0.08$. It is detected by μSR (Ref.25) (marked by the purple dot in the illustration of Fig.4). The doping level $x = 0.08$ is a critical doping when the CNF is beginning to be formed. Effectively it is a percolation phase transition (A scaling in the appendix may give a support to this transition). When doping level is above 0.08, the percolation of SO polarons happen and each plane is conductive already. So the effect of spin polarization inside polarons is now very weak and become less important. As a result, the crossover from *n*-MR ($\alpha < 0$) to *p*-MR ($\alpha > 0$) occurs at this critical doping level. Meanwhile, as shown in Fig.2(a) and (b), the as-grown and short-annealed samples show *n*-MR effect. This *n*-MR may be related to the existence of apical oxygen which could induce antiferromagnetic order inside samples[17]. The suppressing of antiferromagnetic order by applied magnetic field could reduce the spin scattering and then give rise to *n*-MR.

Now we move to the second phenomenon: the linear MR, as shown in Fig.1(a) and Fig.3. Till now, several models were proposed to explain the origin of linear MR, such as quantum MR[32], four-terminal resistor network[33], and density-wave transition[34], etc. Based on the assumption of a gapless spectrum with a linear momentum dependence, *Abrikosov* proposed that linear quantum MR exists when system is in the limiting quantum case with electrons only in one Landau level[32]. But in PCCO, of which the properties are similar to LCCO, quantum oscillation only occurs when the magnetic field is above 60 Tesla[35]. Whereas there exists no quantum oscillation below 60 Tesla, which reveals that no Landau levels are formed in very low magnetic field. Consequently, this model cannot explain the phenomenon of linear MR below 15 T in LCCO.

Parish and *Littlewood* present that if the sample is considered as a network consisting of several

four-terminal resistors, the linear MR could be caused by the Hall signal in an inhomogeneous system[33]. In cuprates, both the inhomogeneous distribution of oxygen in the *ab* plane[36] and gradient distribution of apical oxygen along the *c* axis[25] reveal the inhomogeneity of the samples. So in LCCO, there may exist such four-terminal resistors between different CuO_2 planes. The thickness of thin films is associated with *M* units. The width of films is associated with *N* units. In this situation, in some small area within samples, the current paths perpendicular to the applied voltage gives rise to Hall signal. Especially, the Hall signal is along the current direction and contributes to the MR dramatically as $B \perp I$. This situation is similar to our result: the linear MR is more obvious when we only consider the case of $B \perp I$ (shown in the inset of Fig.3). Near 35 K, the Hall signal near optimal doping level x = 0.1 is almost linear with magnetic field[22,37]. Meanwhile, in lightly doped regime, both the ARPES[38] and Hall effects[37] show that there exists single electron band on the Fermi surface. So LCCO films with x = 0.1 and x = 0.06 at 35 K exhibit linear MR, similar to the situation in non-magnetic silver chalcogenides[39]. Consequently, the four-terminal resistor network gives a plausible interpretation on linear MR in LCCO. But the origin of linear MR with different signs at x = 0.06 and 0.1 in LCCO as well as the similar results in other systems[14,15,26] reported above is still unclear. Since gradient distribution of oxygen[25], both holes and electrons move in the same direction along the four-terminal resistor between different CuO_2 planes. Different kinds of carriers (electrons at x = 0.06 and holes at x = 0.1) give rise to Hall coefficients with different signs. And the Hall coefficients with different signs will contribute to linear MR with different signs. However, this may be one plausible interpretation. To understand linear MR with different signs, it needs further investigation.

Otherwise, since the breakdown of the weak-field Jones-Zener expansion, the linear MR is also verified to exist near the density wave (DW) transition where the Fermi surface is reconstructed and exhibits a local radius[34]. In LCCO, there may exist spin density wave (SDW) transition near the optimal doping level(ref.22). So the DW transition may be another plausible interpretation for the linear MR. However, because the calculation near the DW transition is taken as $B \perp ab$ plane[34], this origin needs further investigation.

In conclusion, we present a thorough study on the in-plane MR of LCCO thin films with the variation of Ce doping and oxygen content. By varying Ce doping, the crossover from *n*-MR to *p*-MR in the normal state occurs near the boundary of long-range antiferromagnetic order. The similar crossover is also observed by changing annealing process. In the lightly Ce doped regime, optimally annealed samples exhibit *n*-MR, which may be interpreted by the CNF network model reasonably. Intriguingly, in the case of $B \perp I$, negative and positive linear field-dependent MR are observed at x = 0.06 and x = 0.1, respectively. The four-terminal resistor network provides a plausible interpretation on linear MR. Alternatively, linear MR near optimal doping level may be closely related to the DW transition. These observations offer improved understanding and insights into the normal state properties in electron-doped cuprates.

This work was supported by the National Key Basic Research Program of China (2015CB921000, 2016YFA0300301), the National Natural Science Foundation of China (Grants No. 11674374, No. 11474338), the Key Research Program of Frontier Sciences, CAS (QYZDB-SSW-SLH008).

Fig. 1. The doping dependence of in-plane MR of optimally annealed LCCO in the normal state. In the doping level (a) x = 0.06, (b) x = 0.07, n-MR is observed with variation of magnetic field. At higher doping levels (c) x = 0.08, (d) x = 0.1, (e) x = 0.11 and (f) x = 0.15, p-MR is observed in the case of both B // I and $B \perp I$.

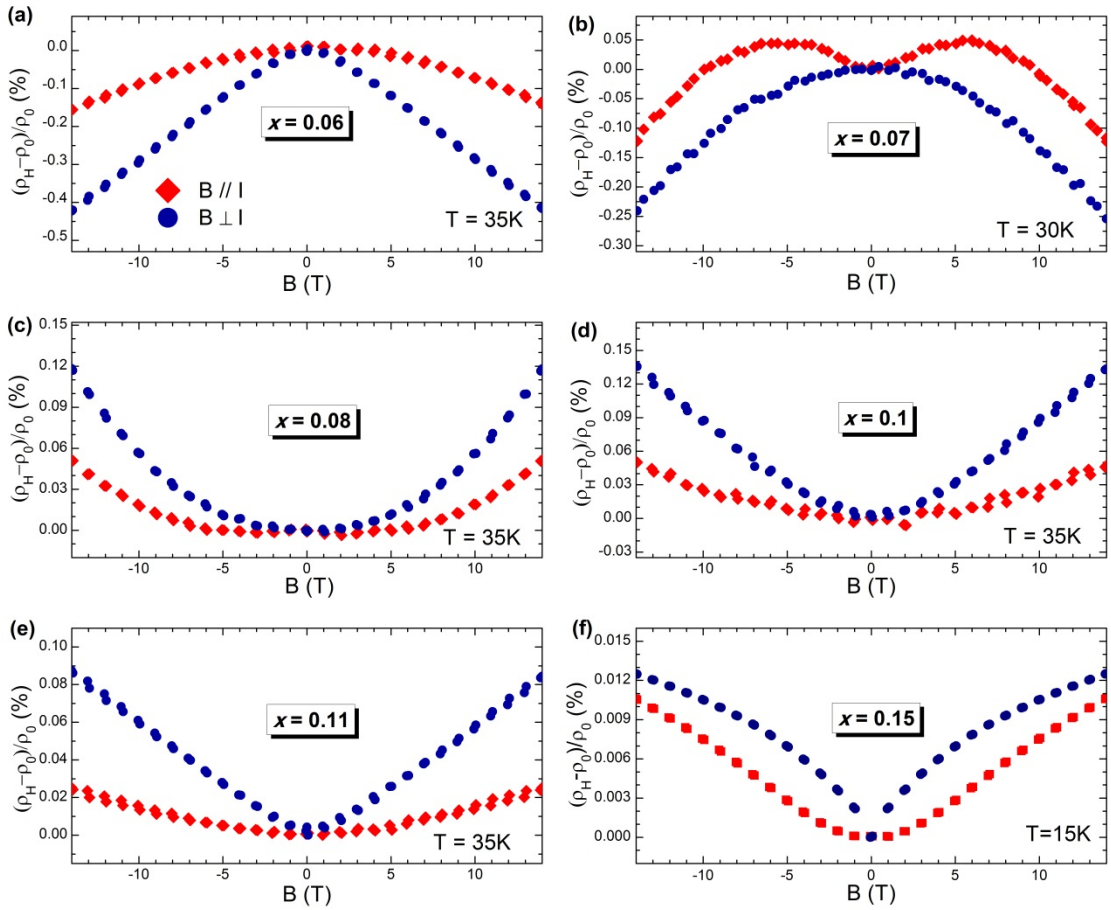

Fig. 2. The oxygen dependence of the in-plane MR at the doping level x = 0.15. When the angle θ between the magnetic field and the current is 0, 45^{o} and 90^{o}, (a) the as-grown films all show n-MR with the variation of magnetic field at T = 10 K; (b) the short-annealed films show n-MR behaviors in the low magnetic field but p-MR above 13 T.

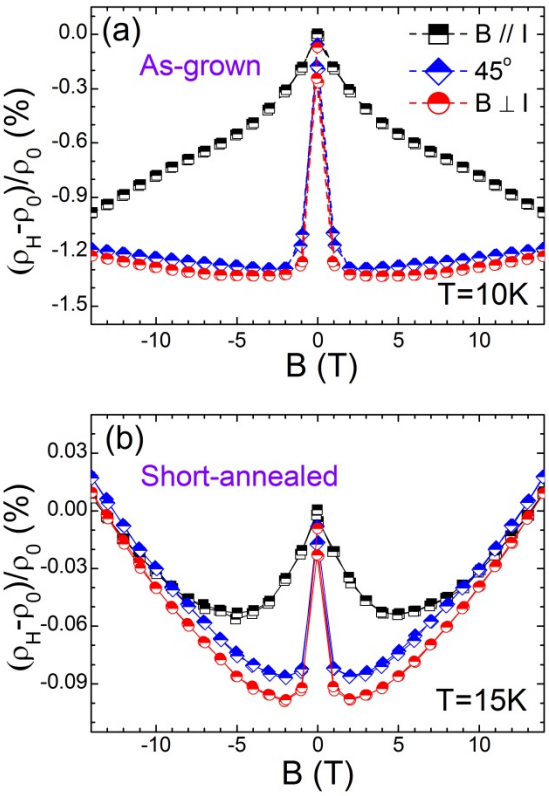

Fig. 3. The linear in-plane MR at the optimal doping level at T = 35 K. When θ = 30°, 45°, 60°, and 90°, the in-plane MR is linear with the magnetic field. The illustration shows the normalization of MR: when the magnetic field was normalized by a sine function of the angle θ, the linear in-plane MR converges onto a single straight line.

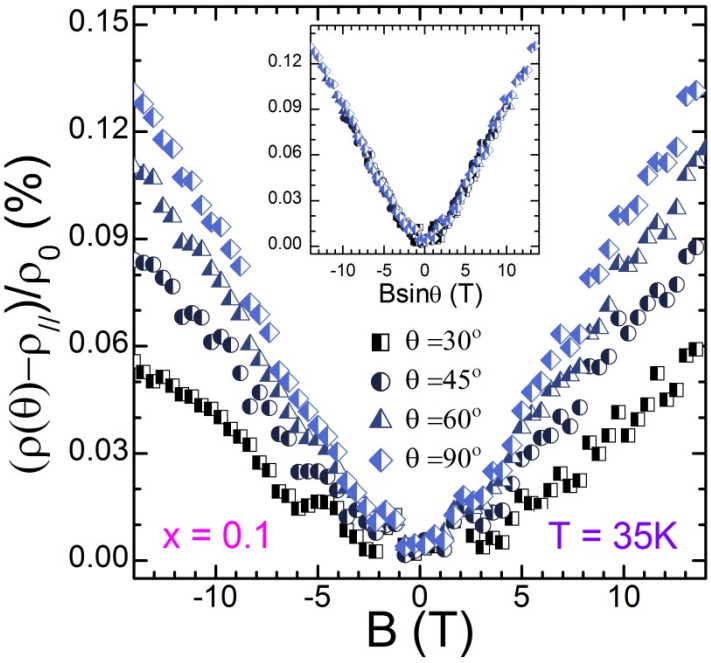

Fig. 4. The phase diagram of the electron-doped cuprate $La_{2-x}Ce_xCuO_4$ achieved by the in-plane MR at T = 35 K. At x = 0.07 and lower doping level, the n-MR is observed. The crossover from n-MR to p-MR occurs between x = 0.07 and 0.08 (marked by the purple dot in the illustration). Above x = 0.08, the p-MR occurs and almost vanishes at the doping level x = 0.15. At the optimal doping level x = 0.1 and underdoped doping level x = 0.06, the linear-in-field MR occurs. The illustration is the temperature-doping phase diagram of $La_{2-x}Ce_xCuO_4$. The boundary of long-range antiferromagnetic order (gray solid line) is achieved by the low energy μSR (ref.25). The light green dash line is the isotherm at 35 K in the phase diagram.

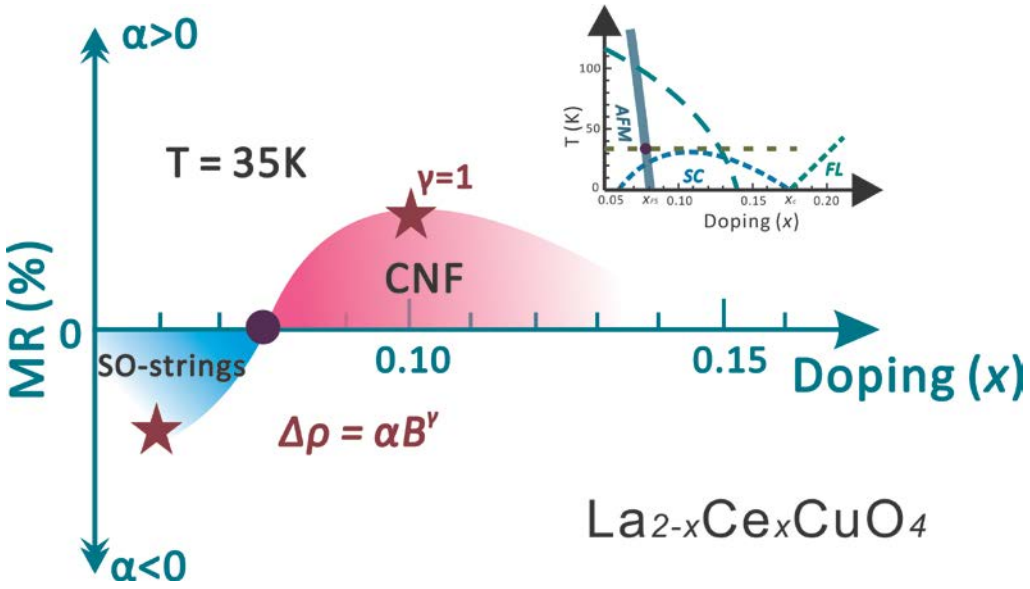

APPENDIX I: A Normalized Scaling

An alternative treatment of the MR involves normalized scaling of the magnetic field (seen in Fig.4). The Fig.1A illustrates the dependence of MR on magnetic field normalized with residual resistivity B/ρ_0 explored for different doping levels x = 0.06 ~ 0.11 at 35 K. The scaling mechanism proposed here may be related to the one underpinning the Kohler's law[40] but rather than varying the temperature, the doping level is varied as the temperature remains constant. In the under-doped regime (x = 0.06, 0.07) the MR remains negative and no universal scaling relation is observed. However, for optimally-doped regime the MR is positive and at low magnetic fields (~ 5 T) a near-linear dependence in the MR versus normalized field B/ρ_0 is seen. In this limited regime of doping and field the MR appear to converge onto a single near-linear function. For larger fields (> 5 T) the scaling relation again breaks down. The contrasting dependence of the scaling relation MR versus B/ρ_0 across magnetic fields at 35 K suggests the presence of multiple field-tuned correlations in the normal state in LCCO films. These observations could have relevance to the presence of SO strings and CNF states, the crossover from *n*-MR to *p*-MR, the enhancement of two-dimensional antiferromagnetic fluctuations, or the formation of Spin Density Wave (SDW) structures.

Fig.1A Normalized scaling MR versus B/ρ_0 is explored for different doping levels at 35 K. In the underdoped regime (x = 0.06, 0.07) no universal scaling relation is seen and the MR remains negative. For optimally doped regime the MR is positive and a near-liner scaling relation emerges at low magnetic fields (~ 5T). Thus, the MR for near optimal doping levels converges onto a single function at fields below 5T. For larger fields strong deviation appears again in the proposed scaling behavior. The contrasting dependence of this scaling behavior across magnetic fields at 35 K suggests the presence multiple field-tuned correlations in the normal state in LCCO films.

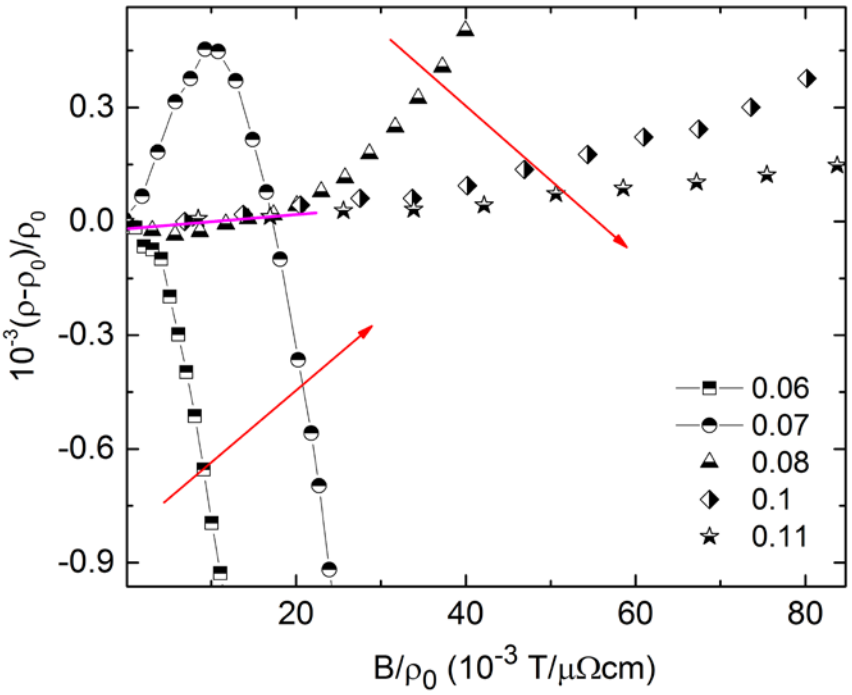

Reference

[1] N. Doiron-Leyraud *et al.*, Quantum oscillations and the Fermi surface in an underdoped high-T_c superconductor. *Nature* **447**, 565 (2007).

[2] B. Vignolle *et al.*, Quantum oscillations in an overdoped high-T_c superconductor. *Nature* **455**, 952 (2008).

[3] R. A. Cooper *et al.*, Anomalous Criticality in the Electrical Resistivity of $La_{2-x}Sr_xCuO_4$. *Science* **323**, 603 (2009).

[4] N. P. Butch, K. Jin, K. Kirshenbaum, R. L. Greene and J. Paglione, Quantum critical scaling at the edge of Fermi liquid stability in a cuprate superconductor. *Proc. Natl. Acad. Sci. USA* **109**, 8440 (2012).

[5] Y. Dagan *et al.*, Origin of the Anomalous Low Temperature Upturn in the Resistivity of the Electron-Doped Cuprate Superconductors. *Phys. Rev. Lett.* **94**, 057005 (2005).

[6] T. Sekitani, M. Naito and N. Miura, Kondo effect in underdopedn-type superconductors. *Phys. Rev. B* **67**, 174503 (2003).

[7] P. Fournier *et al.*, Anomalous saturation of the phase coherence length in underdoped $Pr_{2-x}Ce_xCuO_4$ thin films. *Phys. Rev. B* **62**, 11993(R) (2000).

[8] P. Fournier *et al.*, Insulator-Metal Crossover near Optimal Doping in $Pr_{2-x}Ce_xCuO_4$: Anomalous Normal-State Low Temperature Resistivity. *Phys. Rev. Lett.* **81**, 4720 (1998).

[9] Y. Dagan, M. Qazilbash, C. Hill, V. Kulkarni and R. Greene, Evidence for a Quantum Phase Transition in $Pr_{2-x}Ce_xCuO_{4-\delta}$ from Transport Measurements. *Phys. Rev. Lett.* **92**, 167001 (2004).

[10] K. Jin, X. Zhang, P. Bach and R. Greene, Evidence for antiferromagnetic order in $La_{2-x}Ce_xCuO_4$ from angular magnetoresistance measurements. *Phys. Rev. B* **80**, 012501 (2009).

[11] W. Yu, J. Higgins, P. Bach and R. Greene, Transport evidence of a magnetic quantum phase transition in electron-doped high-temperature superconductors. *Phys. Rev. B* **76**, 020503(R) (2007).

[12] T. Wu *et al.*, Giant anisotropy of the magnetoresistance and the 'spin valve' effect in antiferromagnetic $Nd_{2-x}Ce_xCuO_4$. *J. Phys. Condens. Matter* **20**, 275226 (2008).

[13] A. N. Lavrov *et al.*, Spin-Flop Transition and the Anisotropic Magnetoresistance of$Pr_{1.3-x}La_{0.7}Ce_xCuO_4$: Unexpectedly Strong Spin-Charge Coupling in the Electron-Doped Cuprates. *Phys. Rev. Lett.* **92**, 227003 (2004).

[14] T. Sekitani, H. Nakagawa, N. Miura and M. Naito, Negative magneto-resistance of the normal state in $Nd_{2-x}Ce_xCuO_4$ below T_c and the effect of high magnetic fields. *Physica B* **294**, 358 (2001).

[15] S. Finkelman *et al.*, Resistivity at low temperatures in electron-doped cuprate superconductors. *Phys. Rev. B* **82**, 094508 (2010).

[16] X. Zhang *et al.*, Transport anomalies and quantum criticality in electron-doped cuprate superconductors. *Physica C: Superconductivity and its Applications* **525-526**, 18 (2016).

[17] N. P. Armitage, P. Fournier and R. L. Greene, Progress and perspectives on electron-doped cuprates. *Rev. Mod. Phys.* **82**, 2421 (2010).

[18] J. S. Higgins, Y. Dagan, M. C. Barr, B. D. Weaver and R. L. Greene, Role of oxygen in the electron-doped superconducting cuprates. *Phys. Rev. B* **73**, 104510 (2006).

[19] W. Jiang *et al.*, Anomalous Transport Properties in Superconducting $Nd_{1.85}Ce_{0.15}CuO_{4\pm\delta}$. *Phys. Rev. Lett.* **73**, 1291-1294 (1994).

[20] X. Q. Xu, S. N. Mao, W. Jiang, J. Peng and R. L. Greene, Oxygen dependence of the transport

properties of $Nd_{1.78}Ce_{0.22}CuO_4$. *Phys. Rev. B* **53**, 871 (1996).

[21] S. D. Wilson *et al.*, Evolution of low-energy spin dynamics in the electron-doped high-transition-temperature superconductor$Pr_{0.88}LaCe_{0.12}CuO_{4-\delta}$. *Phys. Rev. B* **74**, 144514 (2006).

[22] H. Yu *et al.*, A conducting nano-filament (CNF) network as a precursor to the origin of superconductivity in electron-doped copper oxides. *arXiv.* **1610**, 04788.

[23] P. Li and R. Greene, Normal-state Nernst effect in electron-doped $Pr_{2-x}Ce_xCuO_{4-\delta}$: Superconducting fluctuations and two-band transport. *Phys. Rev. B* **76**, 174512 (2007).

[24] Y. Dagan, M. M. Qazilbash and R. L. Greene, Tunneling into the normal state of $Pr_{2-x}Ce_xCuO_4$. *Phys. Rev. Lett.* **94**, 187003 (2005).

[25] H. Saadaoui *et al.*, The phase diagram of electron-doped $La_{2-x}Ce_xCuO_{4-\delta}$. *Nature Commun.* **6**, 6041 (2015).

[26] P. Li, F. Balakirev and R. Greene, High-Field Hall Resistivity and Magnetoresistance of Electron-Doped $Pr_{2-x}Ce_xCuO_{4-\delta}$. *Phys. Rev. Lett.* **99**, 047003 (2007).

[27] E. L. Nagaev, Ground state and anomalous magnetic moment of conduction electrons in an antiferromagnetic semiconductor. *JETP Lett.* **6**, 18 (1967).

[28] F. V. Kusmartsev, Formation of Electron Strings in Narrow Band Polar Semiconductors. *Phys. Rev. Lett.* **84**, 530 (2000).

[29] F. V. Kusmartsev, Erratum: Formation of Electron Strings in Narrow Band Polar Semiconductors. *Phys. Rev. Lett.* **84**, 5026 (2004).

[30] F. V. Kusmartsev, About formation of electron strings. *J. Phys.* **9**, 321 (1999).

[31] K. Jin *et al.*, Normal-state transport in electron-doped $La_{2-x}Ce_xCuO_4$ thin films in magnetic fields up to 40Tesla. *Phys. Rev. B* **77**, 172503 (2008).

[32] A. A. Abrikosov, Quantum magnetoresistance. *Phys. Rev. B* **58**, 2788 (1998).

[33] M. M. Parish and P. B. Littlewood, Non-saturating magnetoresistance in heavily disordered semiconductors. *Nature* **426**, 162 (2003).

[34] J. Fenton and A. J. Schofield, Breakdown of Weak-Field Magnetotransport at a Metallic Quantum Critical Point. *Phys. Rev. Lett.* **95**, 247201 (2005).

[35] N. P. Breznay *et al.*, Shubnikov-de Haas quantum oscillations reveal a reconstructed Fermi surface near optimal doping in a thin film of the cuprate superconductor$Pr_{1.86}Ce_{0.14}CuO_{4\pm\delta}$. *Phys. Rev. B* **94**, 104514 (2016).

[36] M. Fratini *et al.*, Scale-free structural organization of oxygen interstitials in La_2CuO_{4+y}. *Nature* **466**, 841-844 (2010).

[37] K. Jin, B. Zhu, B. Wu, L. Gao and B. Zhao, Low-temperature Hall effect in electron-doped superconducting $La_{2-x}Ce_xCuO_4$ thin films. *Phys. Rev. B* **78**, 174521 (2008).

[38] N. P. Armitage *et al.*, Doping Dependence of an n-Type Cuprate Superconductor Investigated by Angle-Resolved Photoemission Spectroscopy. *Phys. Rev. Lett.* **88**, 257001 (2002).

[39] R. Xu *et al.*, Large magnetoresistance in non-magnetic silver chalcogenides. *Nature* **390**, 57 (1997).

[40] J. M. Ziman, Electrons and phonons: the theory of transport phenomena in solids. *Oxford University Press* (1960).